

1 Rios, S., C. Ramos, A. Viana da Fonseca, N. Cruz and C. Rodrigues (2017). "Mechanical and
2 durability properties of a soil stabilised with an alkali-activated cement." European Journal of
3 Environmental and Civil Engineering: 1-23.
4 DOI: 10.1080/19648189.2016.1275987
5 <http://dx.doi.org/10.1080/19648189.2016.1275987>
6

7 **Mechanical and durability properties of a soil** 8 **stabilized with an alkali-activated cement**

9 **Abstract**

10
11
12 Alkali activated cements (AAC) have been extensively studied for different applications as an
13 alternative to Portland cement (which has a high carbon footprint) and due to the possibility of
14 including waste materials such fly ash or slags. However, few works have addressed the topic
15 of stabilised soils with AAC for unpaved roads, with curing at ambient temperature, where the
16 resistance to wetting and drying as well as the mechanical properties evolution over time is
17 particularly relevant. In this paper, a silty sand was stabilized with an AAC synthesized from
18 low calcium fly ash and an alkaline solution made from sodium silicate and sodium hydroxide.
19 The evolution of stiffness and strength up to 360 days, the tensile strength, and the performance
20 during wetting and drying cycles were some of the characteristics analysed. Strength and
21 stiffness results show a significant evolution far beyond the 28th curing day, but still with a
22 reasonable short-term strength. Strength parameters deduced from triaxial tests were found to
23 be very high with stress-strain behaviour typical of cemented soils. Durability properties related
24 to resistance to immersion and wetting and drying cycles were found to comply with existing
25 specifications for soil-cement, giving validity for its use as soil-cement replacement.

26

27 **Keywords:** Fly-ash, Alkali-activated cement, Soil improvement, Resistance to Immersion,
28 Curing time, Durability

29

30 **Introduction**

31

32 In some countries, low cost roads represent a significant percentage of the road network with
33 an important social and economic impact in the local communities. Being sometimes the fastest
34 link between villages and towns, these roads provide access to basic services like health and
35 education, and enable the transport of agricultural goods to markets and raw materials from
36 forest and mines (Brito, 2011; Fukubayashi and Kimura, 2014). However, frequent
37 maintenance works are generally required especially in unpaved roads. This effort can be
38 minimized by the construction of a low cost surface layer of stabilized soil, which uses the local
39 soil instead of the significant resources associated to the construction of a traditional pavement
40 structure (Guedes, 2013).

41

42 Traditionally soils are stabilized with cement and/or lime (Szymkiewicz et al., 2012, Wang et
43 al., 2015, Zhao et al., 2016), however, cement production has severe environmental impacts,
44 using vast amounts of fossil fuels and being responsible for the emission of more than 5% of
45 all the carbon dioxide worldwide (Provis and Deventer, 2014). Hence, the development of low
46 carbon alternative binders using increasing amounts of waste materials has been encouraged
47 (e.g., Consoli et al., 2007). For example, the use of lime and fly ash for soil improvement has
48 been used for decades (Mateos and Davidson, 1962; Ghosh and Subarao, 2001; Consoli et al.,
49 2011), but the activation of fly ash with an alkaline solution is far more effective providing
50 much higher strength (Rios et al., 2016a).

51

52 As first described by Davidovits (1991), geopolymers result from the reaction of a solid
53 aluminosilicate with a highly concentrated aqueous alkali hydroxide or silicate solution. The
54 solid aluminosilicate dilutes in the alkaline solution, which leads to the formation of a gel. Then
55 the system continues to reorganize, as the connectivity of the gel network increases, resulting

56 in the three-dimensional aluminosilicate network associated to geopolymers (Duxson et al.,
57 2007). The results are highly improved if the aluminosilicate source has suffered a previous
58 thermic treatment (Xu and van Deventer, 2003) such as slags, ashes, metakaolin, among others.
59

60 Geopolymers have been studied for different applications within the construction industry,
61 namely looking in detail to the properties of cement, mortars and concrete (e.g., Fernandez-
62 Jimenez et al., 2005; Duxson et al., 2007; Bernal et al., 2011; Abdollahnejad et al., 2015; Tahri
63 et al., 2015). More recently, there are also some works about alkali-activated cements (AAC)
64 for soil improvement applications, where the authors tried to overcome the disadvantages of
65 curing at ambient temperature and the interaction with the local soil. For example, Obana et al.
66 (2012) and Yi et al. (2015) dealt with marine sediments, Sukmak et al. (2013), Cristelo et al.
67 (2011, 2013) and Peirce et al. (2015) worked with clays, and Zhang et al (2013), Rios et al.
68 (2016b) and Phummiphan et al. (2016) used other soils. Depending on the envisaged application
69 and local soil, the challenges are different conversely to what happens in cement, mortars and
70 concrete. For that reason, more research is needed in this area since there are still some issues
71 not completely well understood. Although, a significant improvement in time has been
72 recognized with significant improvements between the 28th and 90th day mark (Rios et al.,
73 2016b), the early age strength and its evolution at long term (after 180 days) is very dependent
74 on the type of aluminosilicate source, type and concentration of alkaline solution and
75 liquid/solids ratio (Messina et al., 2015). Cristelo et al. (2013) showed that there is a strong
76 dependency between the activator/ash ratio and mechanical strength, being an important key
77 parameter for these mixtures.

78

79 This paper pretends to contribute to the increasing knowledge of AAC for soil improvement
80 focusing on the long term behaviour, on the resistance to immersion, and on the resistance to
81 wetting and drying cycles, which are required properties for the specific application of unpaved

82 roads. Moreover, other parameters usually needed in road design were evaluated such as
83 compression and tensile strength, CBR values, and swelling behaviour. For that purpose,
84 existing European standards and specifications developed for soil-cement sub-base layers were
85 used and discussed.

86

87 **Experimental program**

88

89 *Materials*

90 The results presented in this paper concern the stabilization of a Colombian soil classified as a
91 silty sand (SM) according to the unified classification system (ASTM D 2487, 2011). The soil
92 was collected in a quarry site called “El Cajón de Copérnico” located in Soacha in the south of
93 Bogotá. The results of identification tests performed on this soil are summarized in Table 1 and
94 the grain size distribution curve determined by sieving and hydrometer analysis according to
95 ASTM D 422 (1998) is presented in Figure 1. It is a silty sand with non plastic fines, and low
96 sand content, which does not fulfil the Colombian specifications for roads.

97

98 The fly ash (FA) used in the alkaline activation was produced by a Portuguese coal-fired
99 thermo-electric power plant. Its particle size distribution curve (Figure 1) was determined by
100 laser diffraction, using an analyzer from *Beckman Coulter*. Figure 1 also shows the grain size
101 distribution curves of the two mixtures of soil with 10% and 20% of fly ash from which
102 uniformity coefficients (C_U) of 175 and 96 were respectively deduced. This reduction on the
103 uniformity coefficients due to the introduction of fly ash, results in lower Proctor densities as
104 explained further below.

105

106 SEM micrographs of the soil and fly ash particles are shown in Figure 2 (a) and (b) respectively,
107 and the results from EDS semi-quantitative chemical analyses are shown in Table 2. Although

108 both soil and fly ash are composed mainly by silica and alumina, the amorphous structure of
109 the fly ash makes it much more reactive with the alkaline solution, while the soil almost does
110 not take part of the reaction. From the chemical analysis, it is also possible to identify the low
111 calcium content of the fly ash, which was therefore classified as Class F according to ASTM
112 C 618 (2015). EDS spectra was collected during at least 10 minutes using an EDAX equipment.
113 A Dead Time (DT) of 33% was used, with typical 2000 Counts/s. The Live time was 500 s.
114 Quantitative analysis was performed in ZAF standardless mode.

115

116 The alkaline activator solution was made by mixing a commercial sodium silicate (SS) solution
117 ($\text{Na}_2\text{Si}_3\text{O}_7$) with a sodium hydroxide (SH) solution (NaOH) prepared to the desired
118 concentration by dissolving sodium hydroxide pellets in water. The SS solution has a bulk
119 density of 1.464 g/cm^3 at 20°C , a $\text{SiO}_2/\text{Na}_2\text{O}$ weight ratio of 2.0 (molar oxide ratio of 2.063)
120 and a Na_2O concentration in the solution of 13.0%. The SH pellets have a specific gravity of
121 2.13 at 20°C (99 wt%).

122

123 *Mixtures definition*

124

125 The compaction conditions of the treated soil mixtures were based on the modified Proctor tests
126 performed over specimens of soil, fly ash and water. Since Proctor tests give parameters for the
127 compaction of the treated soil immediately after mixing, i.e. without curing, it was considered
128 that the presence of the activator was not very relevant for the purpose of defining the
129 compaction conditions and so the Proctor tests were performed with water. Two fly ash
130 percentages, of 10% and 20% of the dry soil, were adopted and modified Proctor curves were
131 obtained for each case as illustrated in Figure 3. It is clear that the maximum dry unit weight
132 reduced with the amount of fly ash. This can be explained by the uniformity coefficients

133 presented above because well graded soils (with higher C_U values) are able to compact more
134 and therefore achieve higher values of maximum dry unit weight.

135

136 From the results of Figure 3, two sets of mixtures were defined, one with 10% of fly ash (A
137 series) and another with 20% of fly ash (B series) both compacted to their optimum compaction
138 points (10% of FA: $\gamma_d=19.92$ kN/m³ and $w=8\%$; 20% of FA: $\gamma_d=19.53$ kN/m³ and $w=8.8\%$).
139 However, in these new mixtures the liquid phase is no longer just composed by water (as in
140 Proctor tests) but by an alkaline solution. For that reason, in the mixtures preparation the water
141 content was replaced by the liquid content defined as a liquids/solids ratio.

142

143 For each set of mixtures, two sodium silicate to sodium hydroxide ratios (in weight) of 0.5 and
144 1.0 were considered (SS/SH), as well as 4 molal concentrations of sodium hydroxide (5, 7.5,
145 10 and 12.5 molal), comprising 16 types of mixtures. Each mixture was identified as follows:
146 A or B depending on the fly ash content and corresponding compaction point; 05 or 1 depending
147 on the SS/SH ratio of 0.5 or 1.0; and the C5, C7, C10 or C12 depending on the NaOH
148 concentration of 5, 7.5, 10 or 12.5 molal (Table 3).

149

150 Additionally, untreated specimens prepared only with soil and water; or soil, water and fly ash
151 were also moulded for comparison purposes as indicated in the first three lines of Table 3. In
152 this case, an average value of the compaction conditions of these untreated specimens was
153 adopted so that the results could be compared.

154

155 *Specimen preparation and testing procedures*

156

157 The mixture was prepared by mixing the necessary quantities of soil, fly ash, sodium silicate
158 solution, sodium hydroxide pellets and water. Since dissolution of SH pellets in water is a

159 highly exothermic reaction the solution was prepared in the day before to allow sufficient time
160 to cool down to the room temperature. In the moulding day the soil and fly ash were first mixed
161 until complete homogenization and then the activator solution was prepared by mixing the SS
162 solution with the SH solution of the previous day. Finally, the solids (soil and fly ash) were
163 manually mixed with the alkaline solution until a homogeneous paste was obtained.

164
165 The mixture was then statically compacted in a lubricated stainless steel mould of 71 mm of
166 diameter and 142 mm of height according to the procedure described in ASTM D 1632 (2007).
167 Immediately after moulding, the specimens were removed from the mould, and their weight,
168 height and diameter were carefully measured. Before placing the specimen in a controlled
169 temperature room (20°C) for curing, it was wrapped in cling film to avoid moisture loss.

170
171 The experimental plan comprises unconfined compression strength tests (UCS), indirect tensile
172 strength tests (ITS), seismic wave measurements (Waves), Californian Bearing Ratio (CBR),
173 wetting and drying tests (WD), resistance to immersion (IM) and expansion tests (EXP)
174 performed in different curing periods as summarized in Table 4. UCS tests and seismic wave
175 measurements were performed in all the treated soil mixtures for the evaluation of each
176 component effect. The other tests were only performed in some selected mixtures taking into
177 account the UCS and Waves results. Triaxial compression tests (Tx) with local strain
178 instrumentation were performed in the soil, soil+10% of fly ash mixtures without curing, as
179 well as in a selected mixture of treated soil at 28 days of curing period.

180
181 The unconfined compression tests and indirect tensile tests, performed according to ASTM
182 D 1633 (2007) and ASTM D 1634 (1996), respectively, used an automatic load frame with
183 displacement control and a load cell with 25 kN of capacity for specimens up to 28 days of
184 curing and a load cell with 100 kN of capacity for specimens with more days of curing. In order

185 to evaluate the unload-reload stiffness during the UCS tests, small unload-reload cycles at 10%
186 and 25% of the expected maximum strength were performed and local strain instrumentation
187 by means of Hall-Effect transducers was used in all tests. For that reason, the tests were
188 performed at 0.05 mm/min, a slower speed than the indicated in the standard.

189

190 Seismic wave measurements were performed to monitor the curing process by accessing the
191 elastic stiffness increase with time. Being a fast, non-destructive and reliable testing method it
192 allows a good monitoring of a great number of specimens in a feasible time, conversely to
193 strength tests which require a great amount of similar specimens to be tested at different curing
194 periods. It comprises the evaluation of P and S wave propagation times with ultrasonic
195 transducers as described in detail in Rios et al. (2016c). These transducers are more convenient
196 than bender elements (e.g., Ferreira et al., 2011) when used in very stiff materials such as
197 cemented soils (Molero et al., 2011), because it is not necessary to perform a small incision to
198 insert the bender element. Due to the great stiffness and strength of the specimens even with
199 few curing days, an incision with the exact bender size allowing a good coupling was very
200 difficult to execute. Measurements were made at frequencies of 24, 37, 54, 82 kHz and the
201 propagation time was identified in the signal that showed better amplification since it is
202 assumed that wave velocity is frequency independent for the range of frequencies applied (e.g.,
203 Lee and Santamarina, 2005). The equipment set up includes a pair of compression transducers
204 with 82 kHz of nominal frequency, a pair of shear transducers with nominal frequency of 100
205 kHz, a pulse waveform generator and data acquisition unit equipped with an amplifier
206 connected to a personal computer with specific software to operate as an oscilloscope. Test
207 measurements were made along the longitudinal axis of the cylindrical specimen placing the
208 transmitter in the bottom of the specimen and the receiver on the top. To improve the acoustic
209 coupling between transducers and the specimen, ultrasonic conductive gel was used. The results
210 presented below correspond to the average of at least 10 consecutive pulse velocity readings.

211

212 The CBR tests were performed in the Central Laboratory (LABC) of MOTA-ENGIL, which is
213 Quality Certified (n° L0315, 2003) by IPAC (Portuguese Accreditation Institute) in accordance
214 with standard EN ISO/IEC 17025 (CEN, 2005). To obtain the CBR_e values following ASTM
215 D 1883 (1999), three test specimens were prepared according to the previously executed
216 Modified Proctor test, considering the optimum moisture content and compacted with 55, 25
217 and 12 blows, which led to relative compaction levels between 90 and 100%. After a 96h period
218 of saturation, the 3 specimens were subjected to the CBR tests and from these results CBR
219 related with 95% of relative compaction was interpolated. Additionally, immediate CBR tests
220 (CBR_i) were also performed according to NF P 94-078 (AFNOR, 1997). In the case of soil and
221 soil+fly ash mixtures the tests were performed after moulding, while in the case of treated
222 mixtures, the tests were performed at 28 days of curing time.

223

224 The expansion test consisted in a large mould of 152.14 mm of diameter and 100 mm height
225 where the specimen was compacted and its height was monitored during 56 days.

226

227 The wet and drying tests (WD) following NBR 13554 (ABNT, 2012) give an idea of the
228 durability of the material as a capping layer of an unpaved low cost road (Guedes et al., 2015).
229 Following the French specification for stabilized soils with hydraulic binders in embankments
230 and capping layers (LCPC, 2000), some tests were executed to evaluate the short term strength
231 and the resistance to immersion (IM). As the mixtures showed good behaviour in the immersion
232 tests, another set of tests was performed as described below.

233

234 The triaxial compression tests followed the usual procedure: water percolation up to 150-
235 300 ml; saturation up to 500 kPa of back-pressure at a rate of 30 kPa/h; consolidation at
236 30 kPa/h up to the desired effective confining pressure, and shear controlled by displacement

237 in a load frame equipped with a load cell of 10 kN for the tests with unbounded soil and 50 kN
238 for the tests with "treated soil".

239

240 **Results**

241

242 *Unconfined compression and tensile strength*

243

244 The 16 mixtures specified in Table 3 were subjected to unconfined compression strength tests
245 at 28 days to evaluate the best composition for this particular soil. Three specimens of each
246 mixture were moulded and tested in order to have 3 strength measurements for each case. The
247 results presented in Figure 4 show a considerable increase in strength comparing to unbound
248 soil specimens. Mixtures containing 10% of fly ash (A series) have generally lower strength
249 than the mixtures with 20% of fly ash (B series) but are less expensive. In fact, an integrated
250 analysis of cost and strength was made to evaluate the best mixture, which is also expressed in
251 Figure 4. The cost is also associated to the carbon footprint, as higher fly ash content results in
252 a higher quantity of activator, which is more expensive and produces more greenhouse
253 emissions. Giving these results, two mixtures from the less expensive series (10% of fly ash)
254 were selected for the following tests: A05C7 and A1C7. They are both with 7.5 molal
255 concentration because the 5 molal did not show very good results indicated by a higher scatter
256 and some fissures in the specimens that do not give confident results, and the other
257 concentrations are more expensive and do not show a significant increase in strength.

258

259 In fact, in Figure 4 there is no direct correlation between the SH concentration and the UCS as
260 it was expected from other published works (e.g., Xu and van Deventer, 2000; Cristelo et al.,
261 2012). Alonso and Palomo (2001) and Hwang and Huynh (2015) have also reported some
262 decrease in strength for NaOH concentration higher than 10 molal especially for low curing

263 temperatures, as it was the case of this study. Alonso and Palomo (2001) state that high activator
264 concentrations produce high pH in the liquid phase which favours anionic forms of silicate
265 delaying polymerization while if the stable form was the molecular one (ortosilicic acid) the
266 polymerization reaction is favoured. Consequently, since higher concentrations may delay the
267 polymerization process this reduction in strength with increasing concentration might be less
268 evident when higher curing periods are considered. For that reason, some specimens (A1 series
269 – 10% of fly ash and SS/SH = 1) prepared with different NaOH concentrations (7.5; 10 and
270 12.5 molal) were tested at 90 days of curing period. The results showed that the strength
271 reduction with the increase of the molal concentration was also significant at 90 days (46%
272 reduction) and even higher than at 28 days (30% reduction), conversely to what was expected
273 from the literature. This reduction may be due to the alkali activated compositions used in this
274 research study with low values of liquid/solids ratio in comparison with other published works
275 from the literature working with soil-geopolymer mixtures cured at ambient temperature
276 (Zhang et al., 2013; Cristelo et al., 2012, 2013). For this reason, further studies on their
277 controlling variables are still needed since these are very much dependent on the type of mixture
278 and curing conditions.

279
280 The UCS strength of the two selected mixtures was analyzed up to 360 days of curing as
281 illustrated in Figure 5. Both mixtures show a good adjustment with a logarithmic law indicating
282 that it is still evolving at 360 days. This continuous evolution with time, even beyond the 28
283 days reference, is the main difference of this binder in comparison with Portland cement as
284 expressed by Rios et al. (2016b). In fact, the cementation between particles is clearly visible in
285 SEM micrographs of treated specimens. Figure 6 presents the comparison between a treated
286 specimen (A1C7) after 1 year of curing, with a similar specimen where the activator was
287 replaced by water (i.e., uncemented), so the effect of the alkaline activator on the cementation
288 can be properly observed. While the uncemented specimen shows the fly ash particles (with a

289 very rounded shape as presented in Figure 2b) just placed above the soil particles, in the treated
290 specimen there is a clear bond between both materials. Please note that both micrographs of
291 Figure 6 have the same scale for comparison purposes.

292

293 The results of indirect tensile strength tests are presented in Table 5 for the two selected
294 mixtures: A05C7 and A1C7. Despite the two outliers (1 and 5), the relationship between
295 indirect tensile strength and unconfined compression strength is around 7.5% for both mixtures,
296 being a bit smaller than what has been observed in soil-cement tests (around 10% as reported
297 by Rios and Viana da Fonseca, 2013).

298

299 These results allowed the comparison of this material behaviour with the classification chart
300 proposed in LCPC (2000) and EN 14227-10 (CEN, 2006) based on the tensile strength and
301 Young modulus. The tensile strength (R_t) was obtained, as indicated in this guide, by
302 multiplying the indirect tensile strength reported in Table 5 by 0.8. The Young modulus (E)
303 was obtained from the first unload-reload cycle performed in the UCS tests assumed to be
304 elastic. Figure 7 shows the lines that separate the different classification zones for each standard.
305 Although the tested mixtures do not fit within the higher classification zones with more tensile
306 strength and stiffness, their performance is accepted as stabilized material for a capping layer.
307 Please note that the selected mixtures were not the most well performing of Figure 4, so it is
308 possible that other mixtures (such as B1C7) could fit in the higher classes. As in any other
309 cemented material, the binder amount determines its cost and performance.

310

311 *Dynamic stiffness evolution with curing*

312

313 The same specimens tested in UCS tests at 28 days presented in Figure 4 were used for
314 measuring P and S wave propagation time with ultrasonic transducers during the curing process.

315 The interpretation to identify the wave travel time (t) is based on time domain approach,
 316 according to Viana da Fonseca et al. (2009). Wave velocities are then calculated dividing the
 317 specimen length (which corresponds to the travel distance) by the corresponding travel time.

318

319 From the elasticity theory it is possible to obtain the maximum shear modulus (G_0), the
 320 constrained modulus (M_0), the Young modulus (E_0) and the dynamic Poisson ratio (ν) according
 321 to the following equations:

$$G_0 = \rho V_S^2 \quad (1)$$

$$M_0 = \rho V_P^2 \quad (2)$$

$$E_0 = 2G_0 (1 + \nu) \quad (3)$$

$$\nu = \frac{\left(\frac{V_P}{V_S}\right)^2 - 2}{2\left(\frac{V_P}{V_S}\right)^2 - 2} \quad (4)$$

322

323

324 Although different mixtures led to distinct stiffness absolute values, the Young modulus
 325 evolution with time has a similar trend in a significant number of specimens following a
 326 logarithmic trendline with similar exponent values, as illustrated in Figure 8. Following these
 327 results, a unique relationship was obtained - equation (5) - normalizing each curve of Figure 8
 328 by the corresponding Young modulus at 28 days (E_0^{28}) as shown in Figure 9. This relationship,
 329 although with some scatter, is very interesting as it is independent of the mixture. Having E_0 at
 330 28 days it is possible to calculate the E_0 for any mixture at a certain age without any more tests.

$$E_0 = E_0^{28} \cdot [0.24 \ln(t) + 0.15] \quad (5)$$

331

332

333 As explained in Table 4, seismic wave measurements were performed for two mixtures up to
 334 360 days of curing time. Although the stiffness increase is very different in the two mixtures,

335 equation 5 adapts fairly well to both of them (Figure 10). The adjustment is almost perfect up
336 to 30 days, which is reasonable since the normalization is done for 28 days. Moreover, it is also
337 clear that for mixture A1C7 the stiffness is still increasing significantly up to 180 days of curing
338 as observed for strength in Figure 5, which is in agreement with previous studies (eg. Rios et
339 al., 2016c).

340

341 Based on the logarithmic law relating the dynamic stiffness evolution with time, a similar
342 procedure was performed for the UCS results presented in Figure 5, which was compared to
343 the dynamic stiffness relation – equation (5) - as presented in Figure 11.

344

345 Taking these results, these two expressions were combined and a unique linear relationship was
346 found between stiffness and strength without the time parameter, indicating that both variables
347 evolve in the same way.

$$\frac{E_0}{E_0^{28}} = 0.55 \cdot \left(\frac{UCS}{UCS_{28}} \right) + 0.4 \quad (6)$$

348

349

350 *Short term strength and Resistance to immersion*

351

352 According to LCPC (2000) the short term strength is evaluated by: the age for which the
353 specimen has enough strength to support traffic considered higher than 1 MPa; and the
354 resistance to immersion at early ages.

355

356 In the first case, the unconfined compression strength should be performed at 7 and 28 days and
357 then the age for 1 MPa of strength is evaluated by interpolation. If the strength at 7 days is
358 higher than 1 MPa, as it was the case, the interpolation should be done between 4 and 7 days.

359 Table 6 shows the results obtained for the two mixtures at 4, 7 and 28 days and the age for UCS

360 of 1 MPa, showing that the specimens have a significant strength after a few days of curing. It
361 is interesting to note that although these mixtures have a very long curing period, as it was
362 illustrated in Figure 5 with a significant evolution of strength up to 360 days, this does not mean
363 that the short term strength is small.

364

365 The resistance to immersion at early ages is evaluated, according to LCPC (2000), by the ratio
366 between UCS_{i60}/UCS_{60} where UCS_{i60} is the unconfined compression strength of a specimen
367 with 28 days of normal curing followed by 32 days fully covered by water, and UCS_{60} is the
368 unconfined compression strength of a specimen with 60 days of normal curing. Although the
369 water has become a bit blurred, both mixtures passed this test, presenting ratios higher than 0.8
370 (0.86 for A05C7 and 1.03 for A1C7) as recommended in LCPC (2000). The behaviour of these
371 mixtures under water was important to evaluate since AAC and hydraulic binders have quite
372 distinct chemical reactions. In soil-cement, Portland cement particles hydrate with water, i.e.,
373 the mixture retains part of the free water becoming part of the cemented mass. In opposition,
374 according to the chemical reactions presented by Xu and van Deventer (2000), AAC release
375 water during their formation, and so their curing in water could be affected. Moreover, the water
376 could dilute the alkaline medium that favours the activation of fly ashes reducing the reaction
377 extent. However, since the specimen was cured for 28 days before being introduced in water,
378 the strength achieved during that period prevented a significant loss induced by the water,
379 indicating that this material is suitable for roads with exposure to rain.

380

381 To evaluate the wetting effect on the specimen's strength at even earlier ages, a comparison
382 between specimens with different curing times and immersion periods is shown in Figure 12.
383 For both mixtures, results are presented for 7, 28 and 60 days. For 7 days, the specimens were
384 not soaked in water. For 28 days there are two UCS values: one without immersion and other

385 corresponding to a specimen soaked at 7 days. For the 60 days, there is also a UCS value without
386 immersion and another corresponding to a specimen soaked at 28 days.

387

388 The unconfined compression strength of the specimens tested at 28 days reduces when they are
389 soaked in water at 7 days indicating that immersion affects the final resistance. In fact, the UCS
390 values of the specimens tested at 28 days but soaked at 7 days, is similar to the UCS values at
391 7 days of normal curing (especially for A05C7), indicating that immersion almost stopped the
392 strength development. However, in the specimens tested at 60 days of curing, the difference
393 between UCS values of immersed and non immersed specimens is not so significant which is
394 explained by the fact that at 28 days the specimens have reached considerable strength that
395 prevents the specimen from being significantly affected by immersion.

396

397 [California Bearing Ratio tests

398

399 a) Additionally, the CBR values performed on the treated and untreated soil can give an
400 idea of the short and long term performance of the material. The results presented in
401 Table 7 show a stiff behaviour of the untreated soil with results of 60%, which decrease
402 significantly with the introduction of fly ash (30 and 22% of CBR, respectively in
403 mixtures with 10 and 20% of fly ash). In the treated mixtures (A05C7 and A1C7) both
404 the usual CBR_e (which includes a 4 days saturation) and immediate CBR (CBR_i) were
405 tested after 28 days of curing period. CBR_e values of the treated soil are higher than the
406 values obtained in soil-fly ash mixtures, but remain lower than the results obtained in
407 the original soil, which reveals that the curing time was not enough to get the strength
408 given by the treatment or, the immersion period had a significant effect on strength. In
409 fact, the analysis of the data reveals a stiffness decrease with the presence of water,
410 which seems to vary with SS/SH ratio. In fact, CBR_e values show an increase in

411 stiffness for higher SS/SH, while for CBRi (without immersion) lower SS/SH ratios
412 result in higher stiffness with more pronounced differences for higher compaction
413 levels.

414

415 *Resistance to wetting and drying cycles and expansion*

416

417 Following NBR 13554 (ABNT, 2012) developed for soil-cement, the weight losses, water
418 content changes, and volume changes (swell and shrinkage) produced by repeated wetting and
419 drying of hardened specimens were evaluated. For each mixture, 3 specimens were moulded:
420 the first was to obtain the changes in water and volume during the wetting and drying cycles
421 while the other two were used to obtain the specimen losses due to brushing stokes with a wire
422 scratch brush. The specimens were placed in water on the 7th day of curing, following cycles of
423 5 h in water and 42 h in oven (71+/- 2°C). The first specimen revealed that, conversely to what
424 happens in soil-cement, the water was not retained in the specimens during the cycles. This is
425 explained by the AAC characteristics described above. The AAC reactions involve loss of
426 water, and therefore the average water retained, as required by the standard, is negative. The
427 other two specimens, that followed the same cycles plus the brushing, also reported loss of
428 mass, which should correspond to the loss of water (like specimen 1) and loss of soil due to
429 brushing. Removing the loss of water suffered by specimen 1, the loss of mass due to brushing
430 can be obtained. The maximum value obtained in both specimens was 1.58% indicating that
431 brushing does not produce significant degradation to the specimen, in agreement with the results
432 obtained by Guedes et al. (2015) in soil-cement specimens. This is surprising because the
433 specimen surface is not very smooth having big soil grains that could be easily removed by the
434 brush. Since the mass loss was not very significant, it means that the alkali activated cement
435 that links the soil particles is relatively strong.

436

437 After performing the cycles, the specimens were dried in the oven (105-110°C) until constant
438 mass, and then tested in unconfined compression, so their strength was compared to similar
439 specimens subjected to normal curing. The results show that the specimens that followed the
440 wetting and drying cycles have higher strength than the ones that followed the normal curing.
441 This was expected since the geopolymeric reactions are highly accelerated with temperature
442 increase (e.g., Sukmak et al., 2013).

443

444 The volume change (evaluated in the first specimen that followed the wetting and drying cycles
445 but not the brushing strokes) was also reduced, below 1.4%, indicating that there is not
446 significant expansion in water or shrinkage due to curing process. However, to have a
447 quantitative evaluation, an expansion test in normal curing conditions was performed in A05C7
448 mixture as described previously. The variation in the specimen height was measured during 2
449 months, but no significant expansion was recorded since the maximum vertical expansion was
450 0.62%.

451

452 *Stress-strain behaviour and strength envelope*

453

454 Triaxial compression tests with local strain measurements by means of Hall-effect transducers
455 were performed in the soil, soil with 10% and 20% of fly ash (without alkaline activator thus,
456 without cementation), as well as in mixture A1C7 at 28 days here identified as “treated soil”.
457 The confining pressures of these tests were 50, 300 and 600 kPa for the tests with soil and, soil
458 with fly ash and 50, 100 and 150 kPa for the tests with “treated soil” in order to avoid damaging
459 the cementation structure.

460

461 As illustrated in Figure 13 for 50 kPa confining pressure, the treated soil shows a very stiff
462 stress-strain curve, conversely to the soil and soil-ash mixtures, associated to a brittle failure

463 followed by strain softening, as it is typical of cemented materials (Rios et al., 2014). This is
464 related to a high degradation rate of the stiffness degradation curve after bound breakage,
465 observed in this particular case by the ratio between the dynamic stiffness modulus (E_0) and the
466 initial secant modulus (E_{sec}), obtained from the triaxial test with smaller confining stress
467 (50 kPa), which is almost constant up to peak: $E_0/E_{sec} = 6088/551 = 11$.

468

469 It is also observed that the addition of fly ash to the soil slightly reduces the peak strength,
470 which might be related to the specimen lower dry unit weight, considered the optimum modified
471 Proctor value illustrated in Figure 3. This lower optimum density is in agreement with the
472 uniformity coefficients (C_u) since these values reduced with the introduction of fly ash as
473 explained above. However, the use of the alkaline solution largely compensates this, since the
474 treated soil has achieved more than ten times the soil (and soil-ash) strength. This is also clear
475 in the obtained strength envelopes presented in Figure 14. The treated soil shows very high
476 angles of shearing resistance due to high dilatancy angles but also a significant increase in the
477 cohesion intercept as a sign of cementation.

478

479 **Discussion**

480

481 An extensive experimental program was developed to analyse the behaviour of a Colombian
482 soil stabilized with AAC. The aim was to evaluate the performance of this material in different
483 curing conditions regarding its possible application in an unpaved road. The evolution of
484 strength and stiffness with time, which is different from the well-known soil-cement due to the
485 chemical reactions involved in the AAC curing process, have consequences in terms of the
486 material performance, which needed a careful study. For that purpose several tests were
487 performed, first in a great number of mixtures and afterwards in mainly two selected mixtures.
488 Instead of selecting the specimens that showed higher strength, weaker mixtures resulting from

489 lower concentrations of the alkaline solution were selected to observe the lower bound
490 limitations of this technique. This is very important because using a low quantity of activator
491 not only reduces the cost of the mixtures but also their carbon footprint. In that sense, distinct
492 tests recovered from specifications and standards available for soil-cement were used to
493 evaluate the short term strength, the resistance to immersion, the resistance to wetting and
494 drying cycles, strength and dynamic stiffness parameters, among others.

495

496 It has been observed that the key variables that, according to other authors (e.g., Xu and
497 vanDeventer, 2000; Rashad and Zeedan, 2011; Cristelo et al., 2012), should rule the AAC
498 performance (such as the NaOH concentration) do not have the same influence in the mixtures
499 reported in this paper. While the literature works report an increase in strength with NaOH
500 concentration, in the present study this was not clear. This may be due to the much lower
501 liquid/solids ratio of these mixtures, making them particularly sensitive to other key variables
502 such as viscosity. In fact, while in grout mixtures, the increase in the concentration of the
503 alkaline solution (affecting viscosity and workability) does not prevent the strength increase; in
504 a much drier mixture, this may have a significant impact. For this reason further studies
505 involving the development of rational dosage methodologies based on well-defined controlling
506 variables as exists for soil-cement (e.g., Rios et al., 2014) are of major importance. In the case
507 of AAC-soil mixtures the key variables may be the solids/liquid ratio, the ratio between ash and
508 activator, or the ratio between the two components of the activator.

509

510 The tests on the resistance to immersion showed that if the material is submerged very early
511 (for example, at 7 days of curing) there is a significant impact on the final strength since it does
512 not evolve much beyond the early age strength value. On the contrary, if the material is
513 submerged in water at larger ages (for example at 28 days) the impact is almost negligible.
514 These results were in agreement with CBR tests, since the CBR_e values were found to be lower

515 than the CBR_i for the treated specimens, especially in the weaker mixtures. This happens
516 because the AAC reactions involve the loss of water from the specimen, which are not favoured
517 when placed under water. On the other hand, it is admitted that the presence of water may
518 reduce the concentration of the alkali ions in the gel changing its properties and its ability to
519 harden. However, in the wetting and drying cycles of NBR 13554 (ABNT, 2012) the loss of
520 strength that the immersion in water at early ages might cause was compensated by the increase
521 in strength caused by the curing periods in the oven. As reported by several authors (e.g.,
522 Duxson et al., 2007), the AAC reactions are very much affected by temperature, being specially
523 accelerated with temperatures above 85°C.

524

525 For the mild temperatures of the laboratory, around 20°C, the strength parameters obtained for
526 the selected mixture in saturated conditions show high angles of shearing resistance and
527 cohesion intercepts typical of cemented materials, high above the values obtained by the soil
528 itself.

529

530 **Conclusions**

531

532 This paper highlights some important properties of a soil treated with AAC, summarized in the
533 following:

- 534 - Although the increase of strength and stiffness in time is very significant, following a
535 logarithmic law far beyond the usual 28 days observed in materials treated with hydraulic
536 binders, the short term strength (7 days) is still above the 1 MPa, considered the necessary
537 strength to support vehicle circulation;
- 538 - Immersion at early ages may affect the curing process, actively reducing the final strength,
539 except if compensated by high temperatures that fasten the curing process;
- 540 - Stress-strain curves and strength parameters are typical of cemented soils.

- 541 - Further studies are needed to evaluate how the key parameters that rule the AAC grouts
542 (such as the activator type and concentration, the Na₂O/ash ratio, the Si/Al ratio, or the
543 solids/liquid ratio) affect the performance of soils treated with AAC. The present results
544 indicate that existing relations may act differently in this case.
- 545 - Although other studies are still needed, the results presented in this paper encourage the
546 use of this material in unpaved roads especially if applied in warmer climates and if
547 compacting the capping layer in the dry season.
- 548 - These technique will be also more competitive in coal producing countries (which have a
549 great amount of fly ash to dispose) and with lack of calcareous materials for cement
550 production.

551

552

553 **Acknowledgements**

554

555 This work was executed under the project ECOLOSO (reference FCOMP-01-0202-FEDER-
556 038899), funded by the European Fund for Regional Development (FEDER), through the
557 Operational Program for Competitiveness Factors (POFC) of the National Strategic Reference
558 Framework (QREN), on the scope of the incentive system for research and technological
559 development. The authors would also like to acknowledge the Chemical Engineering
560 Department of University of Porto, namely Professors Fernão Magalhães and Adélio Mendes,
561 for the use of the Particle Size Analyser; the company Pegop – Energia Eléctrica SA which runs
562 the thermoelectric power plant of Pego, for the supply of fly ash; and the MCTES/FCT
563 (Portuguese Science and Technology Foundation of Portuguese Ministry of Science and
564 Technology) for their financial support through the SFRH/BPD/85863/2012 scholarship, which
565 is co-funded by the European Social Fund by POCH program.

566

567 **References**

- 568 Abdollahnejad, Z., S. Miraldo, F. Pacheco-Torgal and J. B. Aguiar (2015). Cost-efficient one-
569 part alkali-activated mortars with low global warming potential for floor heating systems
570 applications. *European Journal of Environmental and Civil Engineering*, 1-18.
- 571 ABNT NBR 13554:2012 (2012). Soil-cement - wetting and drying tests - Method of test.
572 Associação Brasileira de Normas Técnicas (in Portuguese)
- 573 AFNOR NF P 94-078 (1997). CBR index after immersion. Association Française de
574 Normalisation, Paris, France
- 575 Alonso, S. and A. Palomo (2001). Alkaline activation of metakaolin and calcium hydroxide
576 mixtures: influence of temperature, activator concentration and solids ratio. *Materials Letters*,
577 47(1-2), 55-62. DOI: 10.1016/S0167-577X(00)00212-3
- 578 ASTM D 422 (1998). Standard test method for particle size analysis of soils. ASTM Int. Annu.
579 B. Stand, Vol. 04.08, 1-8.
- 580 ASTM C 618 (2015). Standard specification for coal fly ash and raw or calcined natural
581 pozzolan for use in concrete. ASTM Int. Annu. B. Stand, Vol. 04.02, 1-5.
- 582 ASTM D 1632 (2007). Standard practice for making and curing soil-cement compression and
583 flexure test specimens in the laboratory. ASTM Int. Annu. B. Stand. Vol. 04.08, 1-5.
- 584 ASTM D 1633 (2007). Standard Test Methods for Compressive Strength of Molded Soil-
585 Cement Cylinders. ASTM Int. Annu. B. Stand. Vol. 04.08, 1-5.
- 586 ASTM D 1634 (2000). Standard Test Method for Compressive Strength of Soil-Cement Using
587 Portions of Beams Broken in Flexure (Modified Cube Method). ASTM Int. Annu. B. Stand,
588 Vol. 04.08, 1-5.
- 589 ASTM D 1883 (2016). Standard Test Method for California Bearing Ratio (CBR) of
590 Laboratory-Compacted Soils. ASTM Int. Annu. B. Stand, Vol. 04.08, 1-5.
- 591 ASTM D 2487-2006 (2011). Standard practice for classification of soils and engineering
592 purposes (Unified Classification System), ASTM Int. Annu. B. Stand. Vol. 04.08, 1-5.
- 593 Bernal, S., R. M. Gutiérrez, A. L. Pedraza and J. L. Provis (2011). Effect of binder content on
594 the performance of alkali-activated slag concretes. *Cement and concrete research*, 41, 1-8. DOI:
595 10.1016/j.cemconres.2010.08.017
- 596 Brito, L. (2011). Design methods for low cost roads. PhD thesis submitted to the University of
597 Nottingham, United Kingdom.
- 598 CEN (2005). EN ISO/IEC 17025. General requirements for the competence of testing and
599 calibration laboratories. Comité Européen de Normalisation, Brussels
- 600 CEN (2006). EN 14227-10 - Mélanges Traités Aux Liants Hydrauliques - Spécifications -
601 Partie10: Sol Traité Au Ciment, Comité Européen de Normalisation, Brussels
- 602 Consoli, N., K. Heineck, M. Coop, A. Viana da Fonseca and C. Ferreira (2007). Coal bottom
603 ash as a geomaterial: influence of particle morphology on the behaviour of granular materials.
604 *Soils and Foundations*, 47(2), 361-373. DOI: 10.3208/sandf.47.361
- 605 Consoli, N., Dalla-Rosa, A., & Saldanha, R. (2011). Variables Governing Strength of
606 Compacted Soil-Fly Ash-Lime Mixtures. *Journal of Materials in Civil Engineering*, 23(4), 432-
607 440. DOI: 10.1061/(ASCE)MT.1943-5533.0000186
- 608 Cristelo, N., S. Glendinning and A. Teixeira Pinto (2011). Deep soft soil improvement by
609 alkaline activation. *Ground Improvement*, 164(GI2), 73-82. DOI: 10.1680/grim.900032

610 Cristelo, N., S. Glendinning, T. Miranda, D. Oliveira and R. Silva (2012). Soil stabilisation
611 using alkaline activation of fly ash for self-compacting rammed earth construction.
612 *Construction and Building Materials*, 36, 727-735. DOI: 10.1016/j.conbuildmat.2012.06.037

613 Cristelo, N., S. Glendinning, L. Fernandes and A. Teixeira Pinto (2013). Effects of alkaline-
614 activated fly ash and Portland cement on soft soil stabilisation. *Acta Geotechnica*, 8, 395-405.
615 DOI: 10.1007/s11440-012-0200-9

616 Davidovits, J. (1991). Geopolymers - Inorganic polymeric new materials. *Journal of Thermal*
617 *Analysis*, 37,1633-1656.

618 Duxson, P., A. Fernandes-Jiménez, J. L. Provis, G. C. Luckey, A. Palomo and J. S. J. van
619 Deventer (2007). Geopolymer technology: the current state of the art. *Journal of Materials*
620 *Science*, 42, 2917-2933.

621 Fernández-Jiménez, A., A. Palomo and M. Criado (2005). Microstructure development of
622 alkali-activated fly ash cement: a descriptive model. *Cement and Concrete Research*, 35, 1204-
623 1209. DOI: 10.1016/j.cemconres.2004.08.021

624 Ferreira, C., Viana da Fonseca, A., Nash, D. (2011). Shear wave velocities for sample quality
625 assessment on a residual soil. *Soils and Foundations*, 51(4), 683-692. DOI:
626 10.3208/sandf.51.683

627 Fukubayashi, Y. and M. Kimura (2014). Improvement of rural access roads in developing
628 countries with initiative for self-reliance of communities. *Soils and Foundations*, 54(1), 23-35.
629 DOI: 10.1016/j.sandf.2013.12.003

630 Ghosh, A., & Subbarao, C. (2001). Microstructural development in fly ash modified with lime
631 and gypsum. *Journal of Materials in Civil Engineering*, 13(1), 65-70
632 DOI:10.1061/(ASCE)0899-1561(2001)13:1(65), 65-70.

633 Guedes, S. (2013). Mechanical behavior of soil-cement reinforced with synthetic fibers for low
634 cost roads. PhD thesis submitted to the Federal University of Pernambuco, Recife, Brasil (in
635 Portuguese).

636 Guedes, S., Coutinho, R. and Viana da Fonseca, A. (2015). Criteria to evaluate the cement
637 content in a soil for a pavement base course. *Geotecnia*, 134, 127-145 (in Portuguese)

638 Hwang, C.-L. and T.-P. Huynh (2015). Effect of alkali-activator and rice husk ash content on
639 strength development of fly ash and residual rice husk ash-based geopolymers. *Construction*
640 *and Building Materials*, 101, Part 1: 1-9. DOI: 10.1016/j.conbuildmat.2015.10.025

641 LCPC (2000). Guide technique pour le traitement des sols à la chaux et/ou aux liants
642 hydrauliques. Application à la réalisation des remblais et des couches de forme. (Technical
643 guide for soils treated with lime and cement, In French), Laboratoire Central des Ponts et
644 Chaussées (LCPC/SETRA).

645 Lee, J., Santamarina, J. (2005). Bender elements: Performance and signal interpretation.
646 *Journal of Geotechnical and Geoenvironmental Engineering*, 131(9), 1063-1070. DOI:
647 10.1061/(ASCE)1090-0241(2005)131:9(1063)

648 Mateos, M. & Davidson, D. T. 1962. Lime and fly ash properties in soil-lime stabilization.
649 *Highway Research Board Bulletin* No 335, 40-64.

650 Messina, F., C. Ferone, F. Colangelo and R. Cioffi (2015). Low temperature alkaline activation
651 of weathered fly ash: Influence of mineral admixtures on early age performance. *Construction*
652 *and Building Materials*, 86, 169-177. DOI:10.1016/j.conbuildmat.2015.02.069

653 Molero, M., I. Segura, S. Aparicio and J. V. Fuente (2011). Influence of aggregates and air
654 voids on the ultrasonic velocity and attenuation in cementitious materials. *European Journal of*
655 *Environmental and Civil Engineering*, 15(4), 501-517.

656 Obana, M., D. Levacher and P. Dhervilly (2012). Durability properties of marine sediments
657 stabilised by pozzolan and alkali-activated binders. *European Journal of Environmental and*
658 *Civil Engineering*, 16(8), 919-926.

659 Peirce, S., L. Santoro, S. Andini, F. Montagnaro, C. Ferone and R. Cioffi (2015). Clay sediment
660 geopolymerization by means of alkali metal aluminate activation. *RSC Advances* 5(130),
661 107662-107669.

662 Phummiphan, I., S. Horpibulsuk, P. Sukmak, A. Chinkulkijniwat, A. Arulrajah and S.-L. Shen
663 (2016). Stabilisation of marginal lateritic soil using high calcium fly ash-based geopolymer.
664 *Road Materials and Pavement Design*. DOI: 10.1080/14680629.2015.1132632

665 Provis, J., Deventer, J. van (Eds.). (2014). Alkali Activated Materials: State-of-the-art Report,
666 RILEM TC 224-AAM. Springer.

667 Rashad, A. and Zeedan, S. (2011). The effect of activator concentration on the residual strength
668 of alkali-activated fly ash pastes subjected to thermal load. *Construction and Building*
669 *Materials*, 25(7), 3098-3107

670 Rios, S. and Viana da Fonseca, A. (2013). Porosity/cement index to evaluate geomechanical
671 properties of an artificial cemented soil. Proceedings of the 18th International Conference on
672 Soil Mechanics and Geotechnical Engineering, 2589-2592, Paris

673 Rios, S., Viana da Fonseca, A. and Baudet, B. (2014). On the shearing behaviour of an
674 artificially cemented soil. *Acta Geotechnica*, 9(2), 215-226, DOI: 10.1007/s11440-013-0242-7

675 Rios, S., Cristelo, N., Miranda, T., Araújo, N., Oliveira, J. (2016a). Increasing the reaction
676 kinetics of alkali activated fly ash binders for stabilisation of a silty sand pavement sub-base.
677 *Road Materials and Pavement Design*, 1-22, DOI: 10.1080/14680629.2016.1251959

678 Rios, S., Cristelo, C., Viana da Fonseca, A., Ferreira, C. (2016b). Structural Performance of
679 Alkali Activated Soil-Ash versus Soil-Cement. *Journal of Materials in Civil Engineering*, 28(2)
680 DOI: 10.1061/(ASCE)MT.1943-5533.0001398.

681 Rios, S., Cristelo, C., Viana da Fonseca, A., Ferreira, C. (2016c). Small and large strain
682 behavior of soil-geopolymer versus soil-cement. *International Journal of Geomechanics* doi:
683 10.1061/(ASCE)GM.1943-5622.0000783

684 Sukmak, P., S. Horpibulsuk and S.-L. Shen (2013). Strength development in clay-fly ash
685 geopolymer. *Construction and Building Materials*, 40, 566-574. DOI:
686 10.1016/j.conbuildmat.2012.11.015

687 Szymkiewicz, F., A. Guimond-Barrett, A. L. Kouby and P. Reiffsteck (2012). Influence of grain
688 size distribution and cement content on the strength and aging of treated sandy soils. *European*
689 *Journal of Environmental and Civil Engineering*, 16(7), 882-902.

690 Tahri, W., Z. Abdollahnejad, J. Mendes, F. Pacheco-Torgal and J. B. de Aguiar (2016). Cost
691 efficiency and resistance to chemical attack of a fly ash geopolymeric mortar versus epoxy resin
692 and acrylic paint coatings. *European Journal of Environmental and Civil Engineering*, 1-17.

693 Viana da Fonseca, A., Ferreira, C., and Fahey, M. (2009). A Framework Interpreting Bender
694 Element Tests, Combining Time-Domain and Frequency-Domain Methods. *Geotechnical*
695 *Testing Journal*, 32(2), 1-17, DOI: 10.1520/GTJ100974.

696 Wang, D., N. E. Abriak and R. Zentar (2015). One-dimensional consolidation of lime-treated
697 dredged harbour sediments. *European Journal of Environmental and Civil Engineering*, 19(2),
698 199-218.

699 Xu, H. and J. S. J. van Deventer (2000). The geopolymerization of alumino-silicate minerals.
700 *International Journal of Mineral Processes*, 59, 247-266.

701 Yi, Y., C. Li and S. Liu (2015). Alkali-Activated Ground-Granulated Blast Furnace Slag for
702 Stabilization of Marine Soft Clay. *Journal of Materials in Civil Engineering*, 27(4), DOI:
703 10.1061/(ASCE)MT.1943-5533.0001100

704 Zhang, M., H. Guo, T. El-Korchi, G. Zhang and M. Tao (2013). Experimental feasibility study
705 of geopolymer as the next-generation soil stabilizer. *Construction and Building Materials*, 47,
706 1468-1478. DOI: 10.1016/j.conbuildmat.2013.06.017

707 Zhao, H., K. Zhou, C. Zhao, B.-W. Gong and J. Liu (2016). A long-term investigation on
708 microstructure of cement-stabilized handan clay. *European Journal of Environmental and Civil*
709 *Engineering*, 20(2), 199-214.

710

711

712

Tables

713
714
715
716
717
718
719
720
721
722
723
724
725
726

Table 1. Physical properties of the soil

Plastic Limit (W_P)	NP
Liquid Limit (W_L)	NP
Mean effective diameter (D_{50})	0.20 mm
Specific gravity (G)	2.64
Fines content (<0.074 mm)	27.9 %
Uniformity Coefficient (C_U)	210
Curvature Coefficient (C_C)	8.60
Maximum dry unit weight for modified Proctor compaction effort (γ_d^{opt})	20.13 kN/m ³
Optimum water content for modified Proctor compaction effort (w^{opt})	8.6 %

Table 2. Composition of the soil and fly ash (wt%)

Element	SiO ₂	Al ₂ O ₃	Fe ₂ O ₃	CaO	K ₂ O	TiO ₂	MgO	Na ₂ O	SO ₃	Others
Soil	80.33	11.41	3.62	-	2.81	0.89	0.27	-	-	0.67
Fly ash	54.84	19.46	10.73	4.68	4.26	1.40	1.79	1.65	0.7	0.5

Table 3. Mixtures composition

Mixture name	% Fly ash	Dry unit weight (kN/m ³)	Liquid content (%)	SS/SH (wt)	SH concentration (molal)
Soil	0	19.86	8.5	0	0
Soil10FA	10	19.86	8.5	0	0
Soil20FA	20	19.86	8.5	0	0
A05C5	10	19.92	8.0	0.5	5
A05C7	10	19.92	8.0	0.5	7.5
A05C10	10	19.92	8.0	0.5	10
A05C12	10	19.92	8.0	0.5	12.5
A1C5	10	19.92	8.0	1	5
A1C7	10	19.92	8.0	1	7.5
A1C10	10	19.92	8.0	1	10
A1C12	10	19.92	8.0	1	12.5
B05C5	20	19.53	8.8	0.5	5
B05C7	20	19.53	8.8	0.5	7.5
B05C10	20	19.53	8.8	0.5	10
B05C12	20	19.53	8.8	0.5	12.5
B1C5	20	19.53	8.8	1	5
B1C7	20	19.53	8.8	1	7.5
B1C10	20	19.53	8.8	1	10
B1C12	20	19.53	8.8	1	12.5

727 Table 4. Experimental plan

Test name	UCS	Waves	UCS and Waves	UCS and Waves	UCS	EXP	CBR	ITS	WD	IM	Tx
Curing time (days)	28	7, 14, 21 and 28	56 and 90	180 and 360	4 and 7	up to 56	28	28	28	(2)	28
Soil	X ⁽¹⁾										X ⁽¹⁾
Soil10FA											X ⁽¹⁾
Soil20FA											X ⁽¹⁾
A05C5	X	X									
A05C7	X	X	X	X	X	X	X	X	X	X	X
A05C10	X	X									
A05C12	X	X									
A1C5	X	X									
A1C7	X	X	X	X	X		X	X	X	X	X
A1C10	X	X	X								
A1C12	X	X	X								
B05C5	X	X									
B05C7	X	X									
B05C10	X	X									
B05C12	X	X									
B1C5	X	X									
B1C7	X	X									
B1C10	X	X									
B1C12	X	X									

728 ⁽¹⁾ In the unbounded soil specimens the tests were performed at 0 days since there is no curing
 729 process

730 ⁽²⁾ Defined in the text

731

732

733 Table 5. Indirect tensile strength tests

Specimen	ITS (MPa)	ITS/UCS
A05C7_1	0.28	10.4%
A05C7_2	0.19	7.0%
A05C7_3	0.21	7.8%
A1C7_4	0.30	7.2%
A1C7_5	0.22	5.3%
A1C7_6	0.33	7.9%

734

735 Table 6. Short term strength: age for UCS = 1 MPa

Mixture	UCS at 4days (MPa)	UCS at 7days (MPa)	UCS at 28days (MPa)	Age for UCS = 1 MPa
A05C7	0.77	1.21	2.70	6 days
A1C7	0.88	1.22	4.17	5 days

736

737

738

Table 7. CBR values

		Untreated soil			Treated mixtures	
		Soil	Soil + 10% fly ash	Soil + 20% fly ash	A05C7	A1C7
CBRe	2.5mm a 95% CR	59%	29%	22%	31%	50%
	5.0mm a 95% CR	61%	31%	23%	28%	51%
	Expansion (95% CR)	0%	0%	0%	1%	1%
CBRi 55 blows	(2.5 mm)	-	-	-	112%	89%
	(5 mm)	-	-	-	116%	94%
CBRi 25 blows	(2.5 mm)	-	-	-	64%	44%
	(5 mm)	-	-	-	65%	47%
CBRi 12 blows	(2.5 mm)	-	-	-	37%	39%
	(5 mm)	-	-	-	38%	37%

739

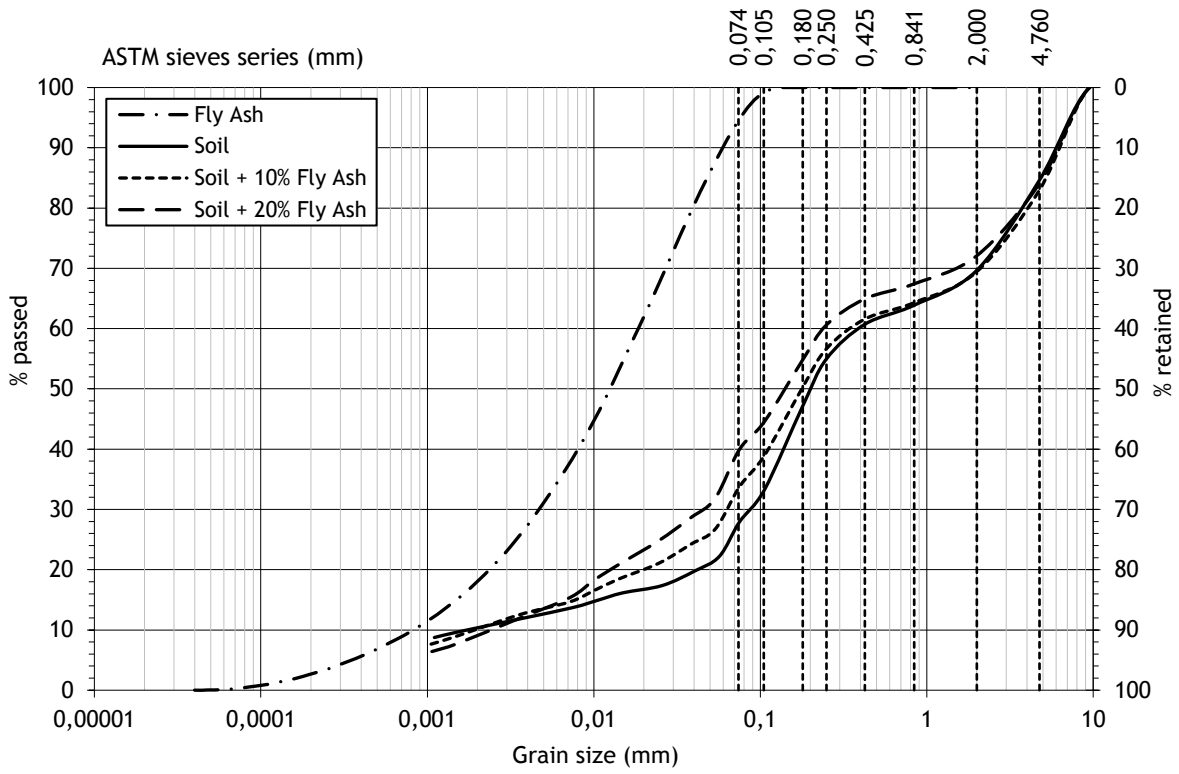
(*) CR means the compaction relative to the Modified Proctor test

740

741

742

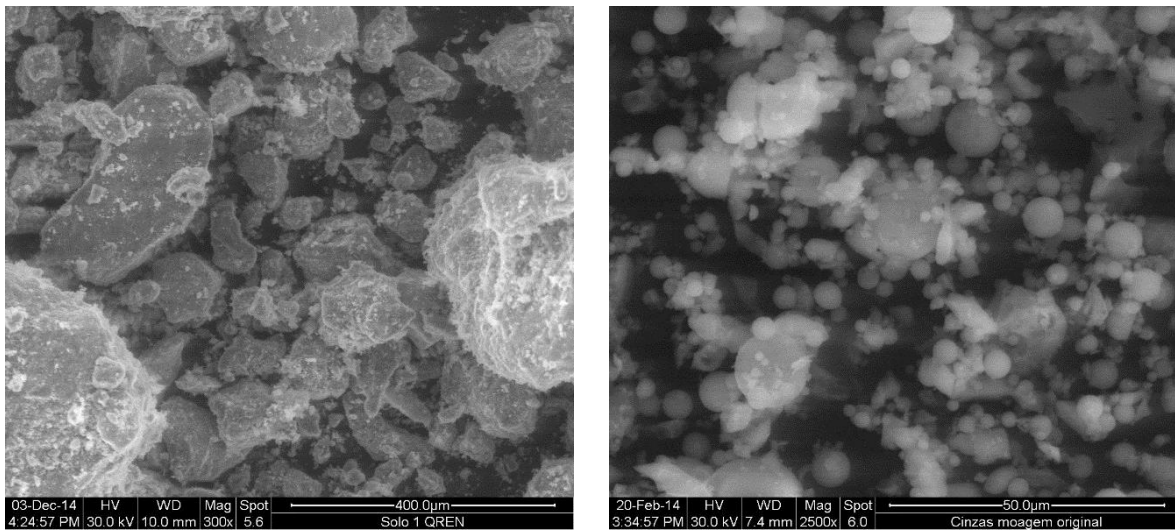
Figures



744

745 Figure 1. Grain size distribution curve of the soil, fly ash and mixtures

746



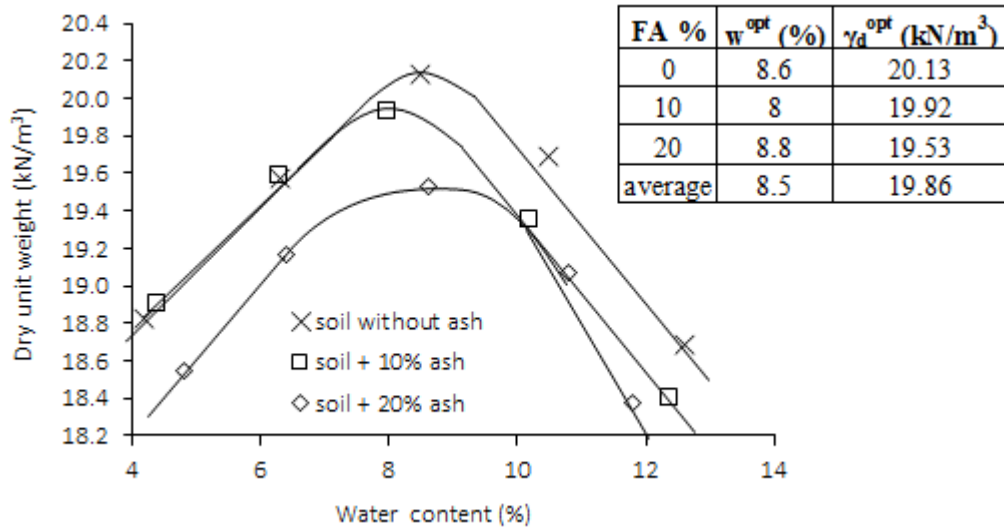
a)

b)

747 Figure 2. SEM micrographs on the particles of soil (a), and fly ash (b),

748

749

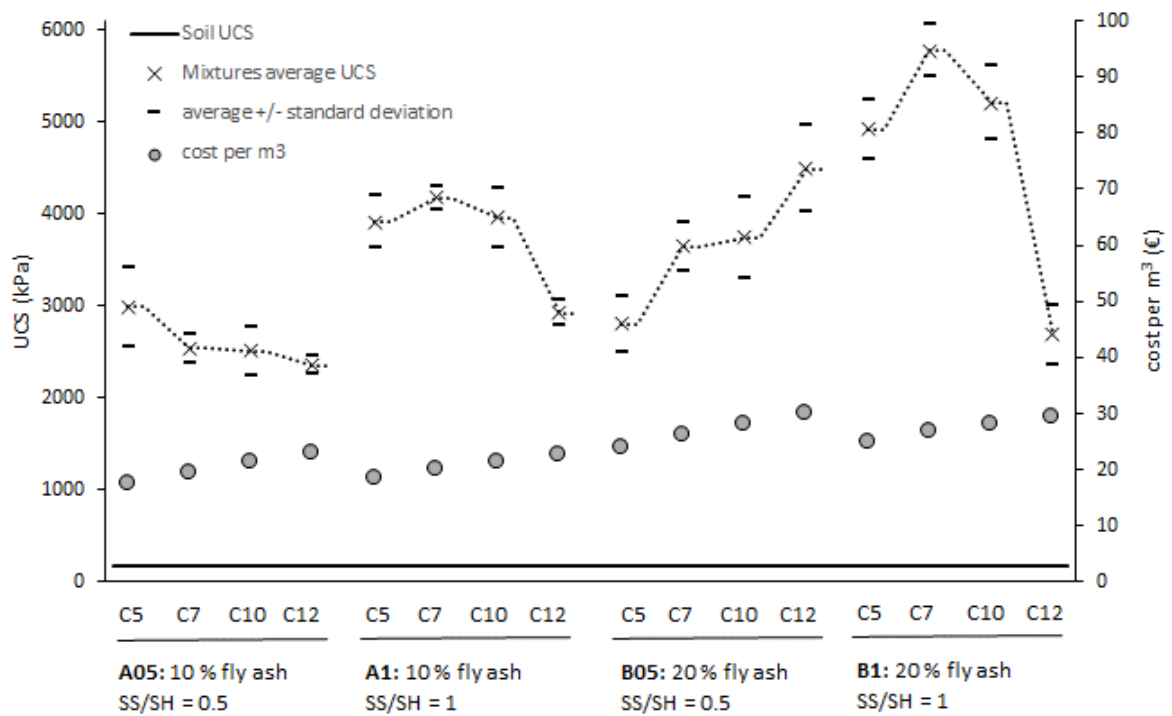


750

751 Figure 3. Modified Proctor curves of the soil, soil+10% of fly ash and soil+20% of fly ash, and
 752 corresponding optimum values

753

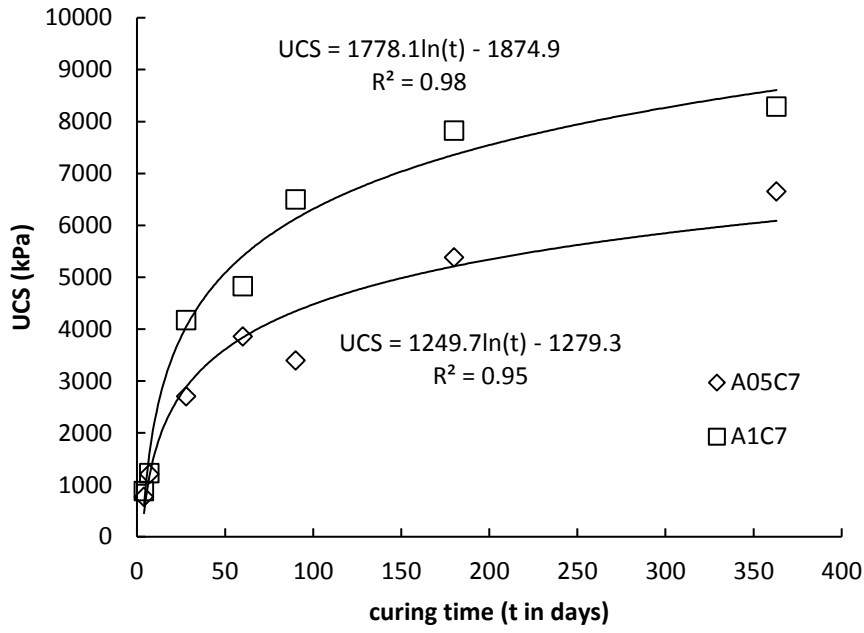
754



755

756 Figure 4. UCS results at 28 days for the 16 mixtures

757



758

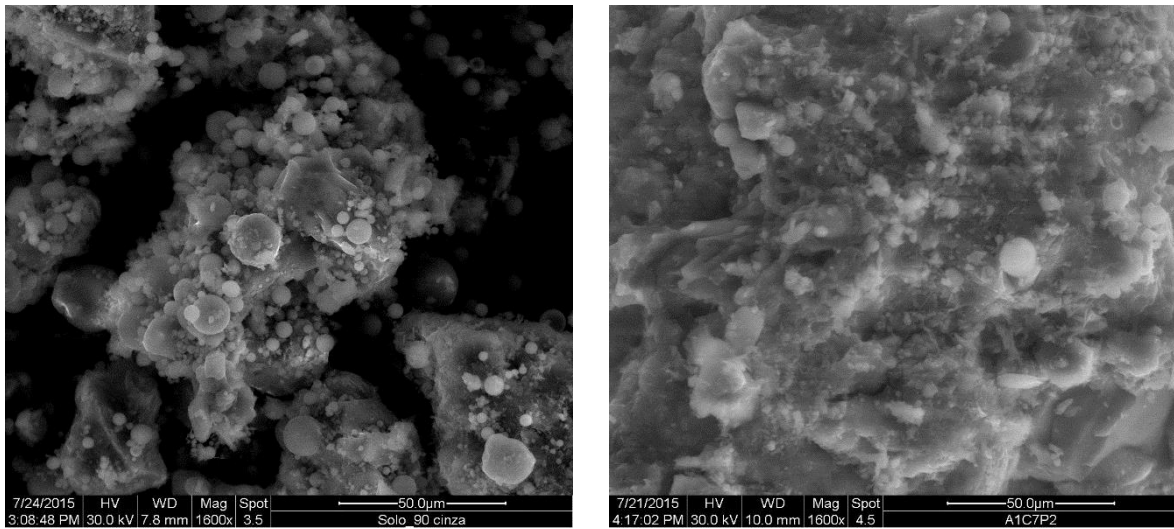
759 Figure 5. UCS results up to 360 days for the two selected mixtures

760

761

762

763



a)

b)

764 Figure 6. SEM micrographs of a mixture of soil and fly ash without activator (a), and mixture of soil,
765 fly ash and activator after 1 year of curing period (b)

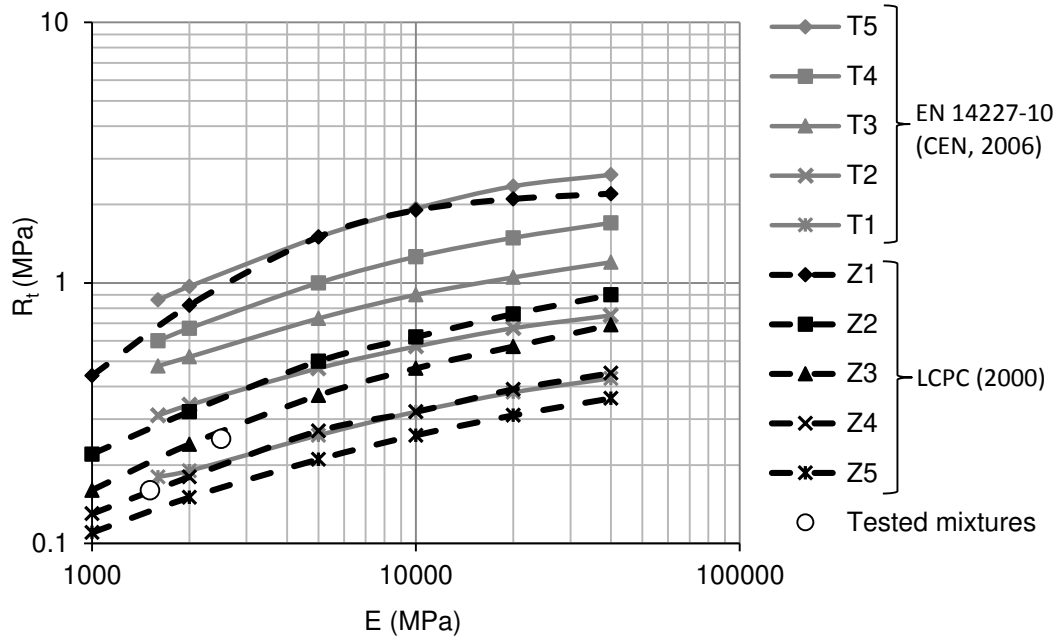
766

767

768

769

770



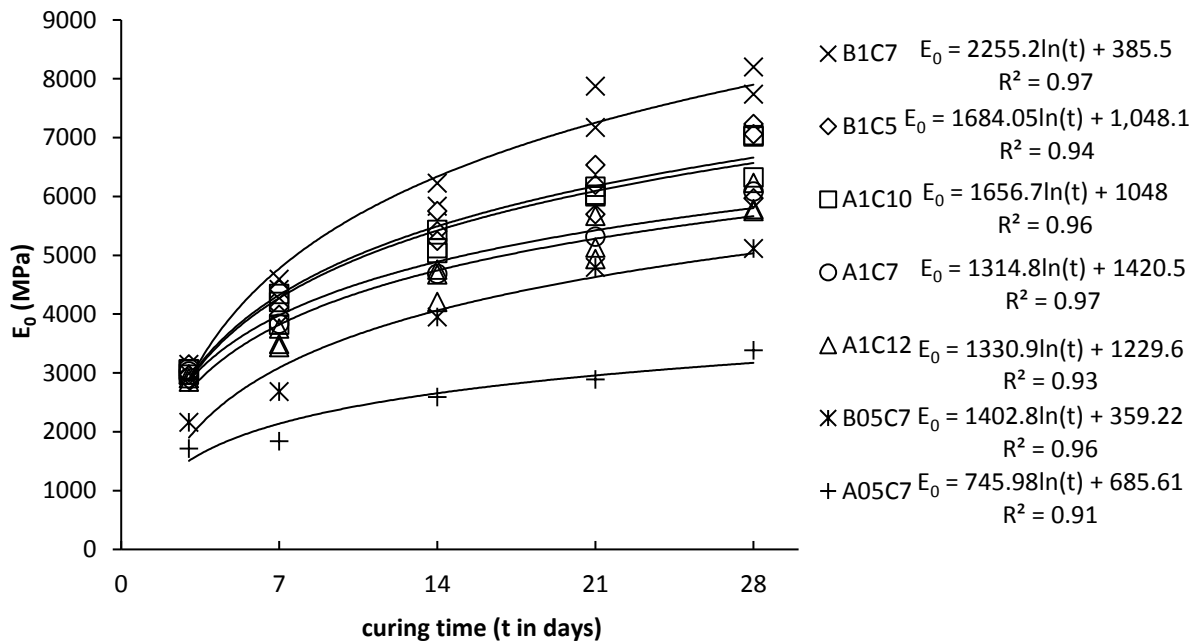
771

772 Figure 7. Material classification zones depending on its stiffness and tensile strength according to EN
 773 14227-10 (CEN, 2006) and LCPC (2000)

774

775

776

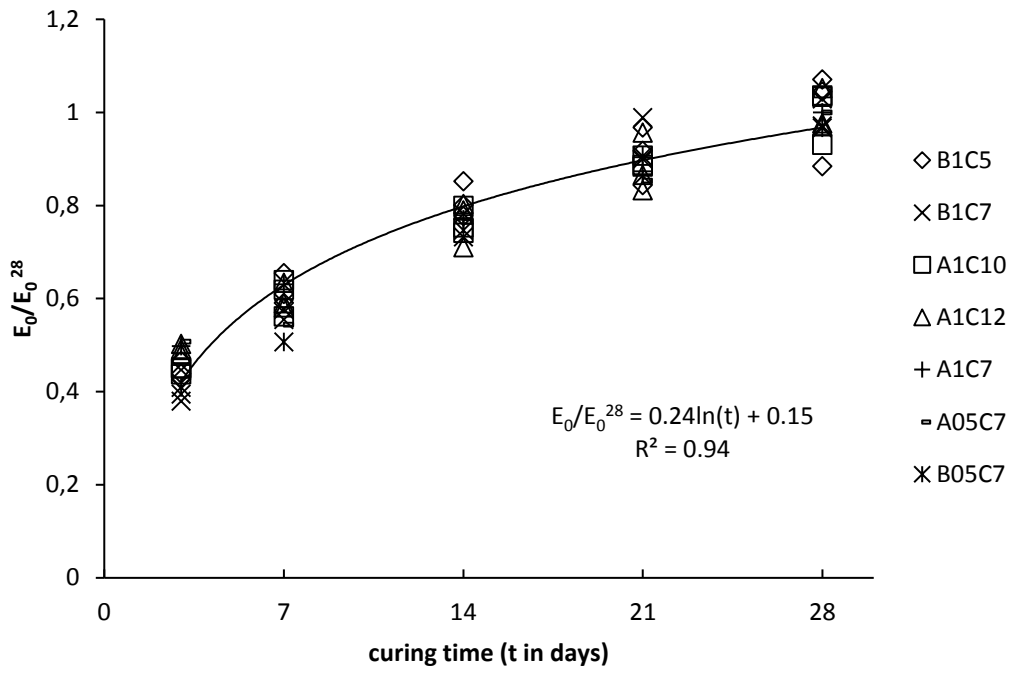


777

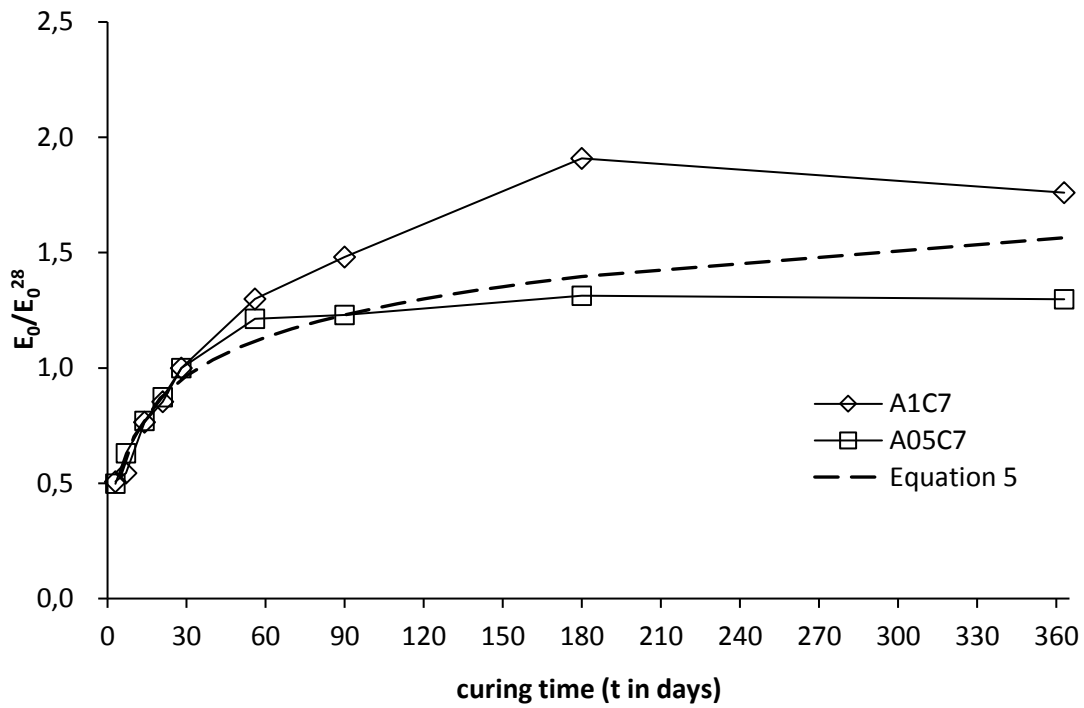
778

779 Figure 8. Young modulus evolution with time for several mixtures

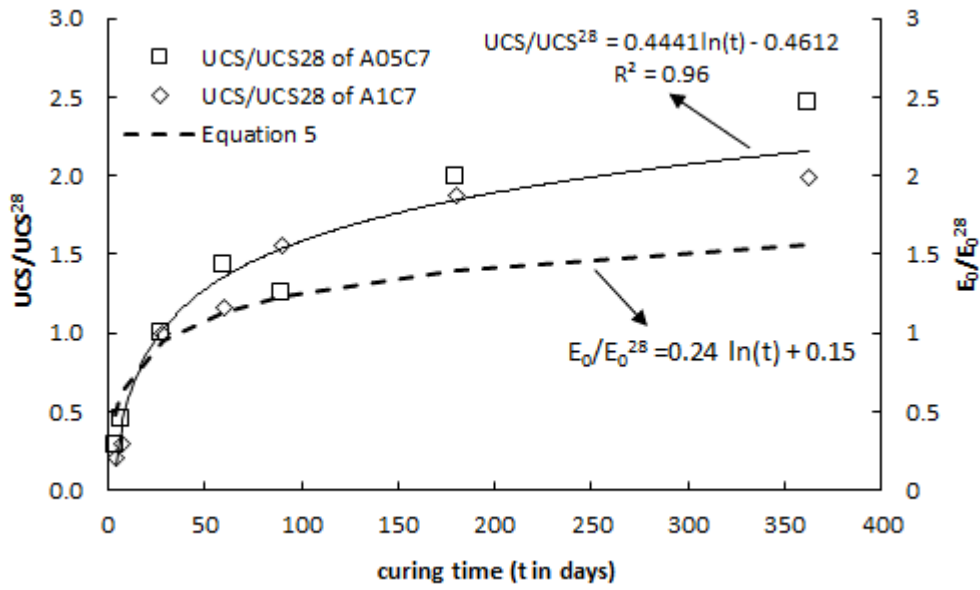
780



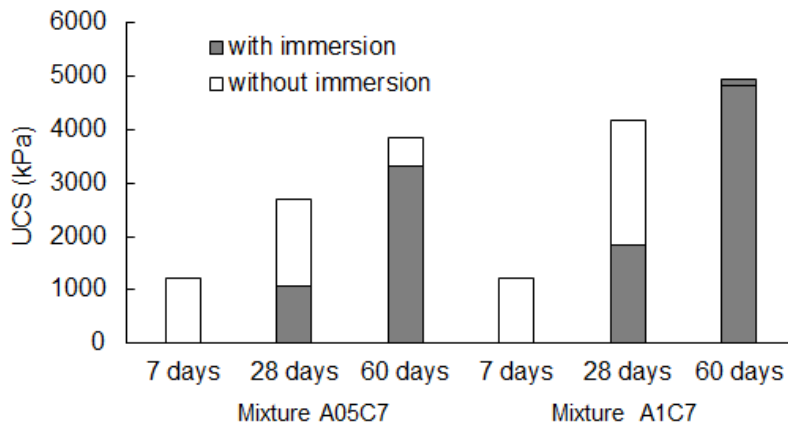
781
782 Figure 9. Normalized Young modulus evolution with time
783



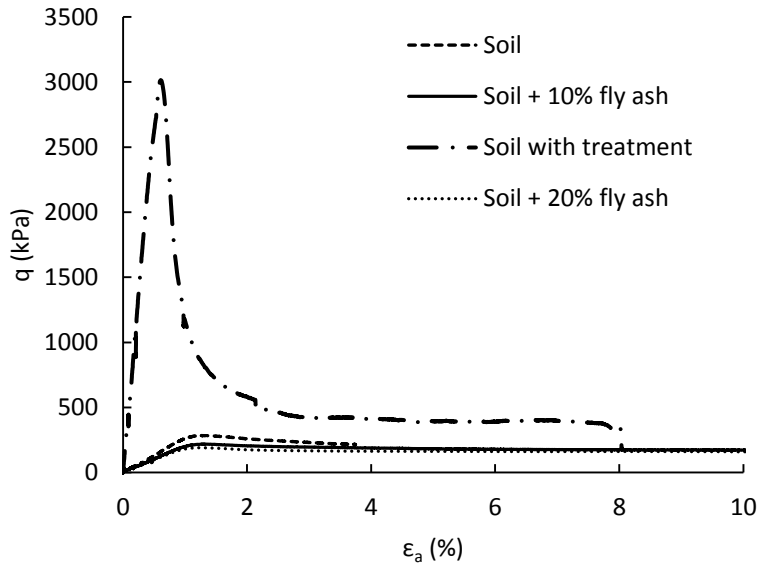
784
785 Figure 10. Young modulus evolution up to 360 days of curing time



786
 787 Figure 11. Strength and stiffness evolution with time
 788
 789



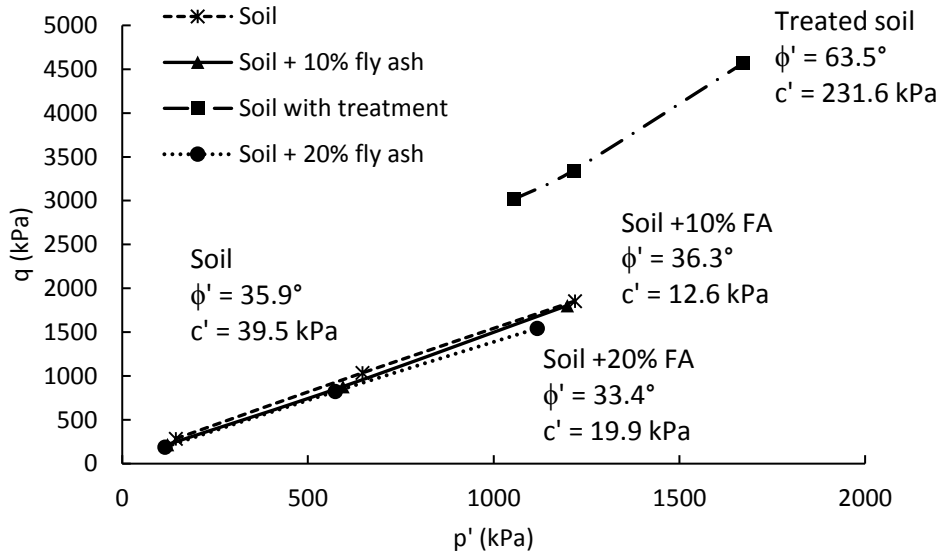
790
 791 Figure 12. Effect of immersion during curing on the unconfined compression strength of two different
 792 mixtures. Note that in the case of specimens tested at 28 days, immersion was performed at 7 days of
 793 curing, while for the specimens tested at 60 days, immersion was at 28 days.
 794
 795



796

797 Figure 13. Stress-strain curves obtained in tested mixtures with and without treatment for 50 kPa of
 798 confining pressure

799



800

801 Figure 14. Strength envelope for the tested mixtures and derived strength parameters

802

803